



REGULAR ARTICLE

Detection of malachite green residue in aquaculture water by using a rare earth fluorescence probe

GUIYU FU^a, HUANYUAN WENG^a, ZHUZHI LAI^b, ZHENGZHONG LIN^{a,*} and ZHIYONG HUANG^{a,c,*}

^aSchool of Food and Biological Engineering, Jimei University, Xiamen 361021, China

^bCollege of Chemistry and Chemical Engineering, Xiamen University, Xiamen 361005, China

^cFujian Key Laboratory of Food Microbiology and Enzyme Engineering, Xiamen 361021, China

E-mail: linzz@jmu.edu.cn

MS received 16 October 2019; revised 16 March 2021; accepted 6 April 2021

Abstract. A rare earth complex Eu(MAA)₃Phen was prepared with methacrylic acid and *o*-phenanthroline as ligands under mild conditions. The complex has a fluorescence emission centered at 618 nm with a half-peak width of 15 nm. Since the emission peak of the complex matches the absorption peak of malachite green (MG), the fluorescence of the complex will be quenched by MG through the fluorescence resonance energy transfer effect. The fluorescence testing conditions for MG were optimized based on fluorescence intensity and fluorescence quenching efficiency. The FRET efficiency was calculated to be 0.21. Under the optimal conditions, the response time was only 5 min. Compared with sulfonamides, chloramphenicol and other banned fishery drugs, the complex exhibited the highest quenching efficiency to MG. The linear range was 0.5–20 μmol L⁻¹, and the detection limit was 117.29 nmol L⁻¹ (3σ/S, n = 9). This complex was used to detect MG residue in aquaculture water, and the recoveries were between 96.10% and 98.76%, indicating that the prepared fluorescent probe could be used for the rapid detection of MG in aquaculture water.

Keywords. Rare earth; Complex; Fluorescent probe; Malachite green; Aquaculture water.

1. Introduction

Malachite green (MG) is a kind of fungicide widely used in the aquaculture industry. However, MG has also been confirmed to be toxic, which will cause mutagenesis, carcinogenesis and teratogenesis after intake by animals or human.¹ Therefore, many countries and regions have prohibited or strictly limited the application of MG. Many businesses have still illegally used MG during aquaculture and transportation because of its low price and good efficiency. In recent years, food safety incidents about MG residues have frequently occurred, resulting in serious health and economic problems. Thus, the daily detection of MG is very necessary.

Currently, the detection methods commonly adopted for MG residues in food mainly include high-performance liquid chromatography,^{2,3} liquid chromatography-mass

spectrometry (LC-MS),⁴ gas chromatography-mass spectrometry (GC-MS),⁵ and surface-enhanced Raman spectroscopy (SERS).⁶ Although these methods have high sensitivity and selectivity, they are limited by the complicated sample pretreatment, cumbersome operation and expensive instruments. Therefore, it is still of great significance to find a rapid and efficient MG detection method.

Quantum dots are a class of fluorescence materials with excellent properties such as wide excitation band, high intensity, easy modification, adjustable luminescence range, high stability and strong anti-bleaching ability. They have been widely used in food analysis. For example, Wu *et al.*,⁷ prepared a fluorescent probe constructed from molecularly imprinted polymer-coated quantum dots for the detection of MG in water and fish with a fluorescence response time of 5 min and detection

*For correspondence

Supplementary Information: The online version contains supplementary material available at <https://doi.org/10.1007/s12039-021-01913-6>.

limit of $0.059 \mu\text{mol L}^{-1}$; Yang *et al.*,⁸ proposed a quantum dot fluorescent probe applied for the analysis of LMG in fish, and the detection limit was 23 nmol L^{-1} ; Cao *et al.*,⁹ developed some water-dispersed quantum dots with high luminescence intensity and light stability for fluorescence detection of MG in water and fish samples, and the detection limit was $1.7 \times 10^{-8} \text{ mol L}^{-1}$. However, quantum dot fluorescence probes are insoluble in water and highly toxic. Rare earth complexes are excellent fluorescent materials with narrow emission peak,^{10,11} long fluorescence lifetime and large Stokes shift. So rare earth complexes are applicable in the analysis of biological molecules and metal ions,¹² and biological imaging.¹³ However, there are few kinds of literature on the application in food analysis field by rare earth complexes, and even no literature was found on the detection of MG residues in food.

In this paper, a rare earth complex, $\text{Eu}(\text{MAA})_3\text{Phen}$, was prepared with Eu^{3+} as the central ion, methacrylic acid (MAA) and *o*-phenanthroline (phen) as the ligands. It was used for the rapid detection of MG residue in aquaculture water based on FRET effect.

2. Experimental

2.1 Reagent

MAA, phen, chloramphenicol, tetracycline and leucomalachite green were purchased from Shanghai Aladdin Biochemical Technology Co. Ltd. Europium oxide, sulfadiazine and sulfaguandine were purchase from Shanghai Macklin Biochemical Technology Co. Ltd. MG were purchased from Sinopharm Group Chemical Reagent Co. Ltd. All the chemicals were in analysis grade.

2.2 Instrument

Thermogravimetry analyzer (SDT Q600, Thermal Analyzers Instruments, USA), Fluorescence spectrophotometer (LS 55, PerkinElmer Ltd, USA), Infrared spectrometer (Nicolet iS10, Thermo Fisher Scientific, USA), Steady-state/transient fluorescence spectrometer (FLS-980, Horiba Fluomax-4, UK) using an uF900 microsecond flashlight, Electrospray ionization Mass Spectrometry (solarix7T, Bruker Daltonics, Germany), X-Ray Powder Diffraction (Ultima IV, Rigaku, Japan).

2.3 Preparation of complex

The preparation of the complex was referred to literatures¹⁴ with some modification. Concentrated

hydrochloric acid (20 mL) and Eu_2O_3 (0.35 g) were mixed and stirred underwater bath for 1.5 h. Ethanol (20 mL) was added to yield a EuCl_3 solution which was further filtered to remove solid impurities. MAA (510 μL), phen (0.36 g) and anhydrous ethanol (20 mL) were mixed in a flask, and the pH value was adjusted to 7 with ammonium hydroxide. The previous EuCl_3 solution in ethanol (20 mL) was added drop by drop under agitation. The mixture was kept at 60°C for a continuous stirring reaction for 4 h. Then, the resulting precipitate was filtered and washed with ethanol several times, and vacuum dried at 50°C for 8 h to obtain the complex powder of $\text{Eu}(\text{MAA})_3\text{Phen}$. The complex powder was dissolved in anhydrous ethanol at 75°C and the solution was transferred to a petri dish covered with a piece of plastic wrap. The wrap was pierced by a pipette nozzle for several holes. Colorless crystalline solid could be obtained after natural evaporation at room temperature for 3–4 days.

2.4 Thermogravimetric analysis (TGA)

The complex of about 6 mg was kept at a heating rate of $10^\circ\text{C}/\text{min}$ under the air atmosphere. Mass changes of the complex were measured by a synchronous thermal analyzer.

2.5 Infrared spectroscopic analysis

The complex and KBr powder were mixed and ground evenly according to the mass ratio of 1:100. The pellet at a thickness of about 1 mm was measured with a Fourier transform infrared spectrometer.

2.6 X-ray powder diffraction and electrospray ionization mass spectrometry

XRD analysis was performed on a Rigaku Ultima IV X-ray diffractometer adopting $\text{Cu-K}\alpha$ radiation (wavelength 1.54 \AA). Electrospray ionization Mass Spectrometry was performed on a Bruker Daltonics solarix 7T with a positive ion model.

2.7 Fluorescence measurement

2000 μL of complex solution (0.03 mg L^{-1}) was added to a centrifuge tube. The solution was added by MG ethanol solution to a final volume of 2050 μL . The fluorescence intensity (F) of the solution at 618 nm was recorded at an excitation wavelength of 295 nm.

The fluorescence intensity of blank solution (F_0) without MG under the same conditions was also recorded. The quenching efficiency, defined as F_0/F , was calculated.

2.8 Aquaculture water sample analysis

Aquaculture water was sampled from a local aquaculture farm. The sample (0.5 mL) was filtered with a filter membrane (0.45 μm). Different concentrations of MG solution in ethanol (0.5 mL) were added to the sample. After dried by nitrogen blow, the residues were dissolved by a quantitative amount of ethanol solution (1 mL) to yield a spiked solution. The spiked solution was further mixed with the complex solution following the previous measurement condition. The fluorescence intensity of the solution was measured to calculate the MG concentration.

3. Results and Discussion

3.1 Synthesis

Acidity is a key factor to influence the coordination reaction. Excessively low pH will result in an incomplete reaction and low yield. However, excessively high pH will lead to the generation of rare-earth hydroxide or other insoluble substances. The previous investigation found that the suitable pH was from 7 to 8. Nevertheless, the target complex was inevitably accompanied by an unsaturated coordination complex which caused unstable fluorescence emission. Therefore, a small amount of ethanol was added to wash the unsaturated coordination complex and reaction reagents several times. The complex was supposed to have a structure as shown in Figure 1.

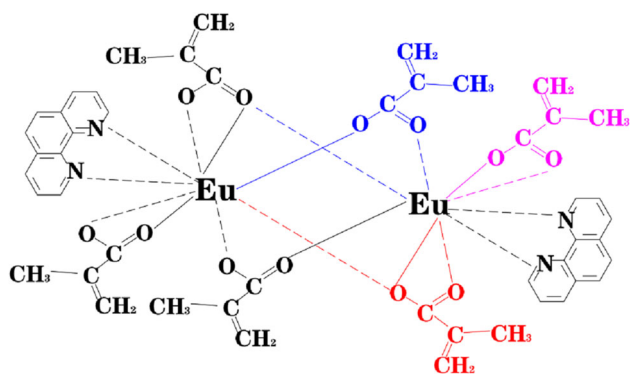


Figure 1. Molecular structure of the complex

3.2 Thermogravimetric analysis and infrared spectroscopic analysis

Thermogravimetric analysis curves of the complex were shown in Figure 2 (left). It could be seen that there was only a slight mass loss from room temperature to 245 $^{\circ}\text{C}$, which might be caused by water molecules adsorbed on its surface. The high decomposition temperature indicated that the complex had good thermal stability. The complex underwent a drastic weight loss from 245 $^{\circ}\text{C}$ to 598 $^{\circ}\text{C}$, which was caused by the removal of organic ligands. The weight loss rate of 71.43% at this stage was close to the theoretical value of 74.11%. After 598 $^{\circ}\text{C}$, the mass remained almost unchanged. The residue was presumably to be Eu_2O_3 with a mass rate of 26.77%, close to the theoretical value of 25.89%. Thermogravimetric analysis further confirmed that the composition of the complex was $\text{Eu}(\text{MAA})_3\text{Phen}$.

The infrared spectrum of the complex was shown in Figure 2 (right). The free MAA molecules had a strong carboxyl vibration peak at 1695 cm^{-1} , which split into 1562 cm^{-1} and 1427 cm^{-1} vibration peaks in the complex. The stretching vibration peak of C=C moved to 1645 cm^{-1} , indicating that MAA was involved in the coordination reaction with europium ions. The C-H out-of-plane bending vibration of benzene ring in phen molecule occurred at 847 cm^{-1} and 666 cm^{-1} . The planar bending vibration shifted from 841 cm^{-1} and 739 cm^{-1} to 780 cm^{-1} and 731 cm^{-1} , respectively, indicating that the lone pair electrons in phen molecules were linked with europium ions *via* coordination bonds.¹⁴ Infrared spectroscopy further confirmed the composition and structure of the complex.

3.3 X-ray diffractions and electrospray ionization mass spectrometry

The compound $\text{Eu}(\text{Maa})_3\text{phen}$ lacked crystallographic data so a compound $\text{Eu}(\text{Crot})_3\text{phen}$ ¹⁵ with a structure similar to $\text{Eu}(\text{Maa})_3\text{phen}$ was cited. A calculated XRD pattern of $\text{Eu}(\text{Crot})_3\text{phen}$ and an experimental XRD pattern of $\text{Eu}(\text{Maa})_3\text{phen}$ were shown in Figure S1 (Supplementary Information). The diffraction peak of $\text{Eu}(\text{Maa})_3\text{phen}$ was at $2\theta=8.16^{\circ}$, 10.34° , 10.82° , 11.14° , 12.84° , 14.62° , 21.98° , 24.62° and 33.04° . The experimental pattern was in good agreement with the theoretical pattern in diffraction angle (2theta) according to Tables S1 (SI), indicating $\text{Eu}(\text{Maa})_3\text{phen}$ was also in a structure motif as $\text{Eu}(\text{Crot})_3\text{phen}$. However, the peak intensities of two XRD patterns were

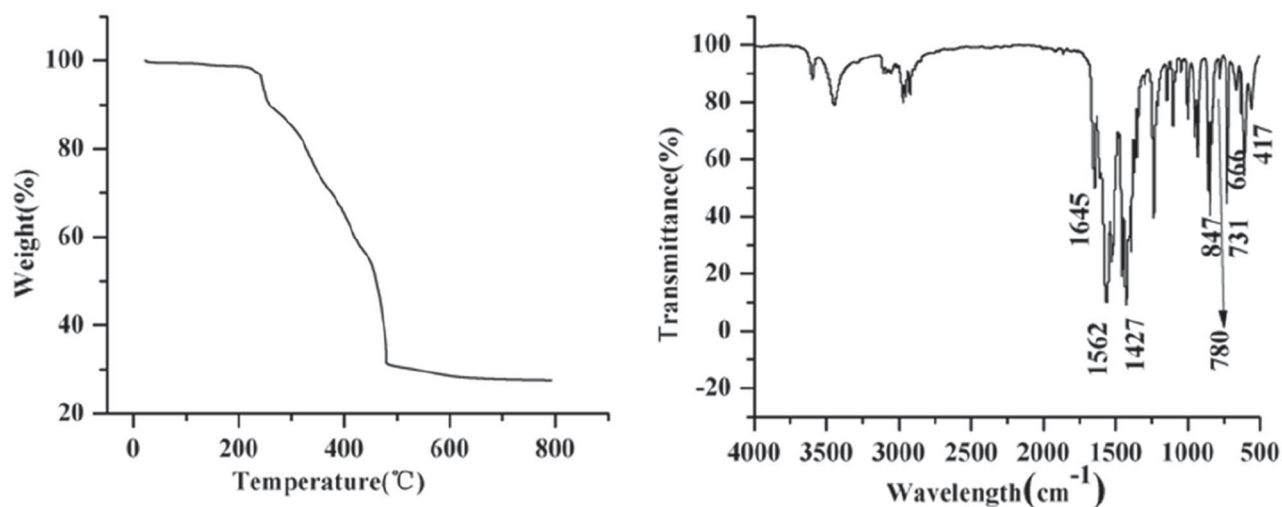


Figure 2. TGA curve of complex (left) and FT-IR spectrum of complex (right)

different which was probably caused by the preferred orientation effect that usually observed in XRD.

The MS measurement result was illustrated in Figure S2 (SI). The peak at 503.04 may be caused by $[\text{Eu}(\text{Maa})_2\text{phen}]^+$ fragment. The peak at 683.11 may be caused by $[\text{Eu}(\text{Maa})_2\text{phen}_2]^+$ fragment. The peak at 909.05 may be caused by $[\text{Eu}_2(\text{Maa})_5\text{phen}]^+$ fragment. The peak at 1089.12 may be caused by $[\text{Eu}_2(\text{Maa})_5\text{phen}_2]^+$ fragment. The peak at 1269.19 may be caused by $[\text{Eu}_2(\text{Maa})_5\text{phen}_3]^+$ fragment. The above possible fragment ions were listed in Table S2 (SI). The MS result further confirmed that the $\text{Eu}(\text{Maa})_3\text{phen}$ complex had a molecular structure illustrated in Figure 1.

3.4 Fluorescence properties

The absorption spectra of complex, MG and mixture in ethanol solution were shown in Figure S3 (SI). The complex exhibited a strong absorption at 260 nm which was caused by LMCT transition. The addition of MG cause slight absorbance decrease. The fluorescence spectra of the complex in ethanol solution (0.03 mg mL^{-1}) were shown in Figure 3 (right). The excitation band of the complex was mainly in the range of 260–320 nm. The highest fluorescence intensity at 295 nm was determined as the excitation wavelength. The main emission peaks of the complexes were located at 596 and 618 nm, which were ascribed to the transition of ${}^5\text{D}_0 \rightarrow {}^7\text{F}_1$ and ${}^5\text{D}_0 \rightarrow {}^7\text{F}_2$, respectively.¹⁶ The intensity of peak at 618 nm was higher than that of 596 nm. Furthermore, the fluorescence at 618 nm was not affected by excitation light due to a wide Stokes shift (324 nm) and a narrow half-peak width (15 nm). These properties were helpful for

the improvement of fluorescent selectivity to receptor molecules.

The fluorescence lifetime measurement was carried out to investigate the fluorescence quenching mechanism. The lifetimes were fitted by a dual exponential equation:

$$R(t) = A + B_1 \exp(-t/\tau_1) + B_2 \exp(-t/\tau_2)$$

$R(t)$ represented the fluorescence intensity at the time of t ; τ_1 and τ_2 were the fluorescence lifetimes. B_1 , and B_2 were the weight values. The detailed fitted values were listed in Table S3 (SI). The average fluorescence lifetime (τ_{av}) was calculated by the following formula:

$$\tau_{\text{av}} = \Sigma B_i \tau_i^2 / \Sigma B_i \tau_i$$

As shown in Figure 3 (left), the fluorescence lifetime of the complex was calculated to be 572.00 μs while the fluorescence lifetime of the mixture (complex and MG) was 450.92 μs . The difference in fluorescence lifetime indicated that the fluorescence quenching of complex by MG was caused by the fluorescence resonance energy transfer FRET.¹⁷ The fluorescence emission of the complex overlaps the absorption of MG. Moreover, the complex and MG were both soluble in the solvent so that the distance between the fluorescence donor and the receptor was short enough for the occurrence of a significant FRET effect. A FRET efficiency of 0.21 was calculated based on the formula of $E = 1 - (\tau_{\text{da}}/\tau_{\text{d}})$, τ_{da} and τ_{d} are the fluorescence lifetimes of the complex in the presence and absence of MG.^{18,19} The quantum yields of the complex before and after interacting with MG at room temperature were determined with Rhodamine B

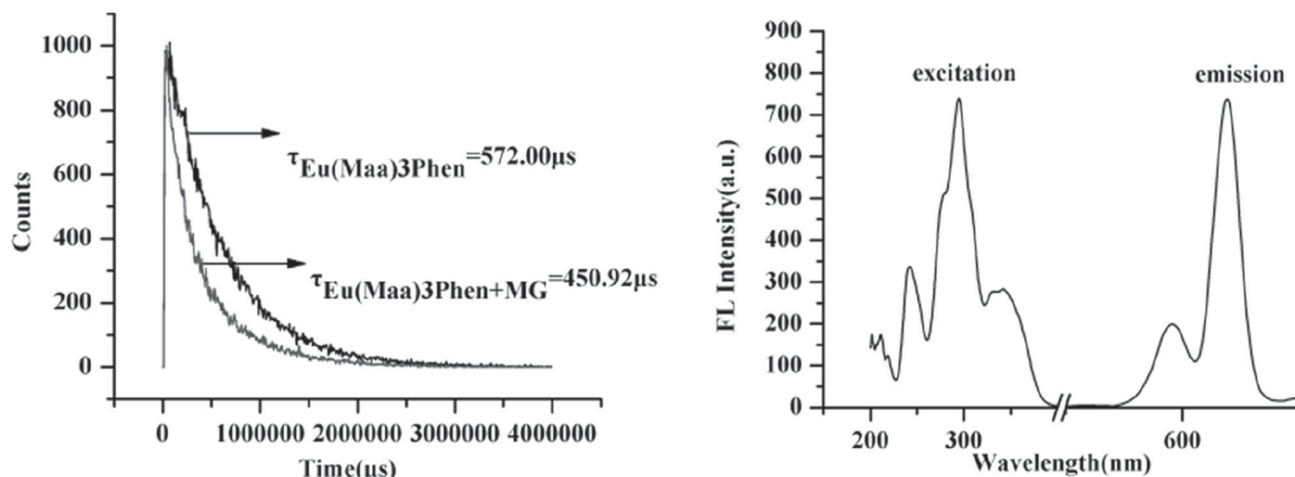


Figure 3. Fluorescence lifetime spectrum of the complex (left); Excitation and emission fluorescence spectra (right). Exciting wavelength was at 295 nm and the emission wavelength was at 618 nm.

as the reference substance at the same excitation wavelength. The detailed information was listed in Table S4 (SI). The quantum yields of the complex before and after interacting with MG was 9.49% and 5.21%. The results were in good agreement with the quantum yield of the Eu(III) complex reported in the literature.²⁰

3.5 Detection condition

Water, dimethyl sulfoxide (DMSO), acetonitrile (ACN), methanol (MT) and ethanol (ET) were used as the solvents, and the concentration of the complex was fixed at 0.03 mg L⁻¹. The effects of the above solvents on F₀ and F₀/F were compared. The results were shown in Figure 4 (left). It can be seen that obvious difference of F₀ or F₀/F in different solvents were observed. The order of F₀ was

water<DMSO<ACN<MT<ET, and the order of F₀/F was water<DMSO<MT<ET<ACN. Water is easy to bind to rare earth metal ions. The presence of O-H bonds, with high vibration energy, will induce fluorescence quenching of the complex. Considering high solubility for the complex, low price and low toxicity, ethanol was selected as the solvent.

The effect of the complex concentration in F₀ and F₀/F was investigated. The results were shown in Figure 4 (right). F₀ increased with the complex concentration while F₀/F first increased and then decreased. So the concentration of the complex was 0.03 mg mL⁻¹.

The experiments at various pH values in various buffer solutions in ethanol were carried out. The results showed that the highest F₀ and F₀/F were observed at pH value of 7.0. But the addition of buffer media caused significant decrease of F₀. Considering the fact that the complex solution and the aquaculture

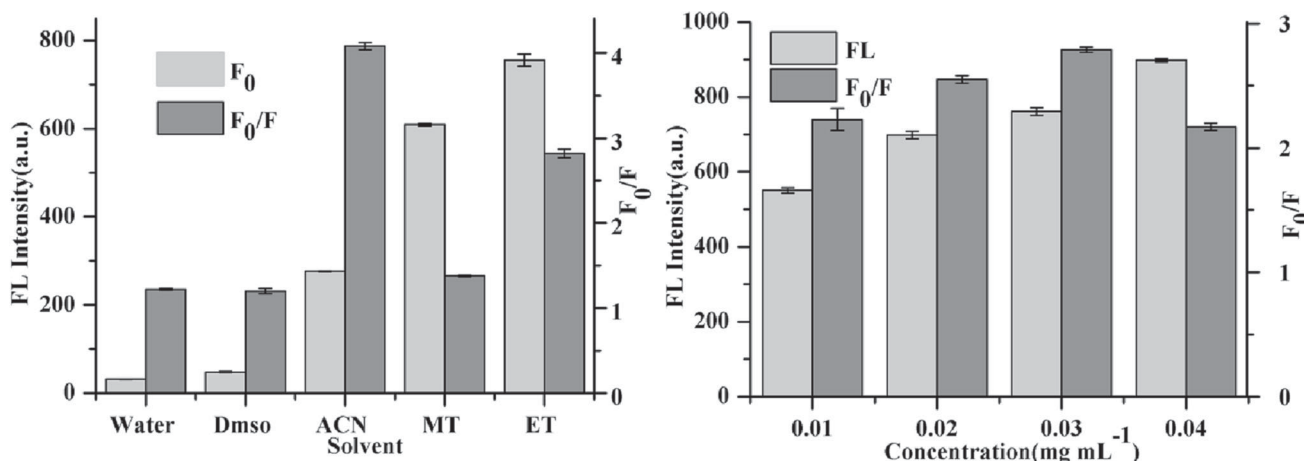


Figure 4. Influence of solvent on F and F₀/F (left); Effect of the complex concentration on F₀ and F₀/F (right)

water sample after treatment were both at neutral pH value, no buffer solution was introduced.

3.6 Selectivity

A metabolite of MG, leucomalachite green (LMG), often coexists with MG. Furthermore, sulfaguanidine (SG), sulfadimethylpyrimidine (SM2), chloramphenicol (CAP) and tetracycline (TC) are some common banned fishery drugs. Therefore, these substances were chosen to investigate the selectivity of the complexes. It could be seen from Figure 5 that this substance also cause fluorescence quenching of the complex to a different extent, but their quenching efficiencies were lower than that of MG, indicating that the complex exhibited a certain selectivity to MG. The maximum absorption peaks of these substances were far from the emission peak of the complexes so that effective FRET would not occur and the quenching efficiencies were not higher than MG. The fluorescence quenching by these substances was probably caused by electron transfer.

3.7 Fluorescence response time

In order to investigate the fluorescence response time of the complex to MG, F_0 (without MG) and F values at an MG concentration of 0.02 mmol L^{-1} from 1 to 30 min were measured. As shown in Figure 6, F_0 values kept constant, implying that the complex was stable. F values decrease in a short time and tend to be stable. Therefore, the detection time of 5 min after sample addition was adopted. The complex and MG

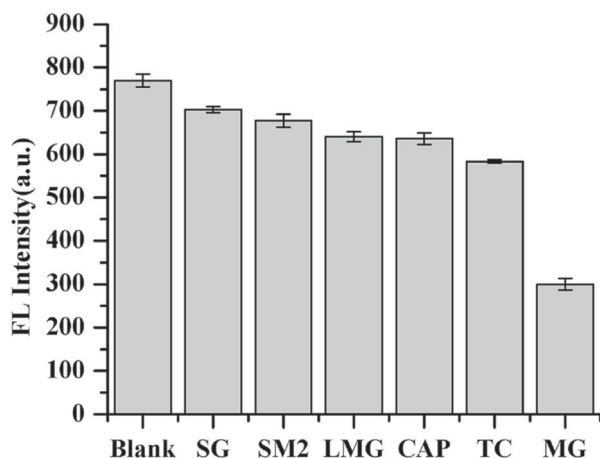


Figure 5. Fluorescence intensity of the complex to SG, SM2, LMG, CAP, TC, and MG (The concentration of each substance was 0.02 mmol L^{-1})

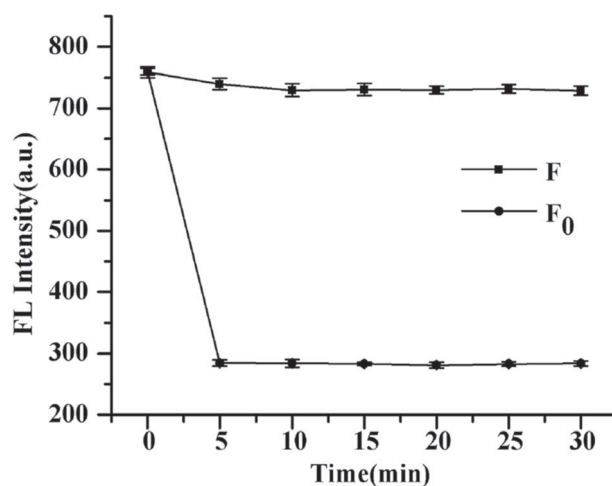


Figure 6. Kinetic curves of the complex with (F) and without (F_0) MG

molecules are soluble in the solvent and were distributed evenly, which provides a rapid and complete interaction between acceptor and receptor. The short fluorescent response time was necessary for the rapid analysis of samples.

3.8 Standard curve

Different concentrations of MG solution were added to the complex in ethanol under optimized conditions, and the fluorescence spectra of the solution before and after the addition of MG were measured after 5 min. The fluorescence spectra were shown in Figure 7 (left). It can be seen from Figure 7 that after the addition of MG an obvious fluorescence quenching was observed under UV light. Fluorescence quenching efficiencies and MG concentration was fitted based on the Stern-Volmer equation,²¹ $F_0/F=1+K_{SV}[C]$. F_0/F represents the fluorescence quenching efficiency, K_{SV} is the quenching constant, and $[C]$ is the concentration of MG. The fitted results were shown in Figure 7 (right). The linear equation was $F_0/F=0.057[C]+0.965$ ($0.5\text{--}20 \text{ } \mu\text{mol L}^{-1}$, $R^2=0.992$) and the limit of detection (LOD) was estimated to be $117.29 \text{ nmol L}^{-1}$ ($3\sigma/S, n=9$). The LOD was higher than that of fluorescent probes based on quantum dots (59 and 17 nmol L^{-1}).^{7,22} Quantum dot was known as a high fluorescence material and the fluorescence probe based on it had a very low LOD.

3.9 Sample analysis

The fluorescence probe was used in the analysis of MG residues in aquaculture water to investigate its

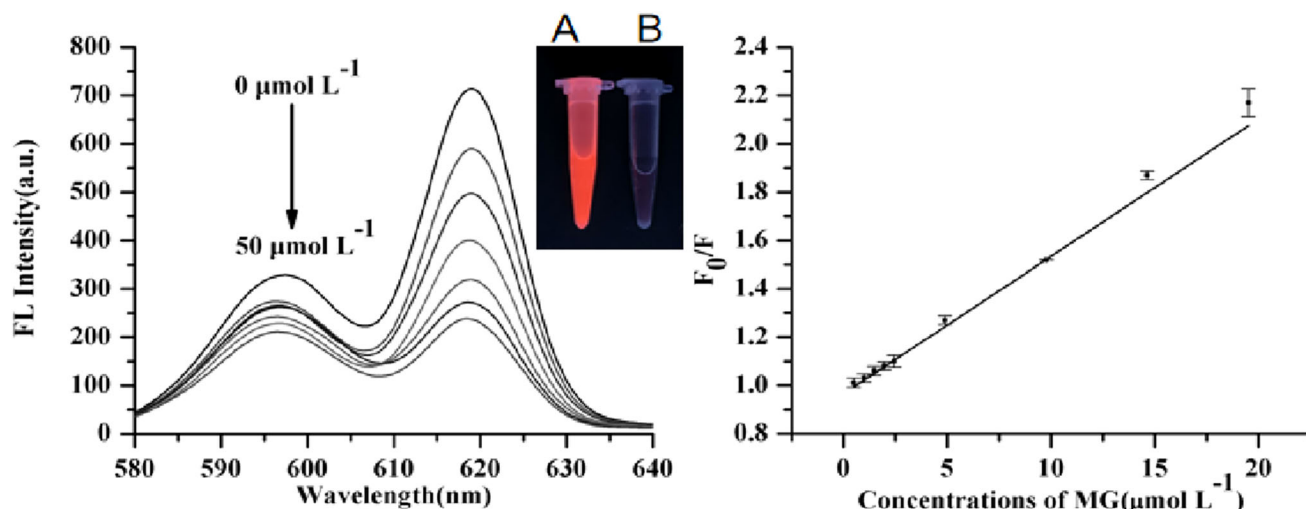


Figure 7. Fluorescence spectra of the complex and MG at different concentration (left) and Linear relationship between F_0/F and MG concentration (right). Inset shows visual fluorescence emission under UV light for complex (A) and Complex-MG (B)

Table 1. Results of MG recovery in cultured water

Sample	Spiked level ($\mu\text{mol L}^{-1}$)	Measured value ($\mu\text{mol L}^{-1}$)	Recovery (%)
Aquaculture water	1	0.96 ± 0.04	96.10
	5	4.94 ± 0.12	98.76
	10	9.79 ± 0.08	97.92
	20	19.35 ± 0.17	96.73

applicability. The results were shown in Table 1. It could be seen that the standard recoveries of MG in aquaculture water were in a range of 96.10–98.76%, and the relative deviation is lower than 4.2%. The results showed that the complex was practical for rapid and accurate analysis in the real sample in spite of various interfering substances.

4. Conclusions

A rare earth complex $\text{Eu}(\text{MAA})_3\text{Phen}$ was prepared with a fluorescence emission at 618 nm. The fluorescence of the complex was quenched quantitatively by MG based on the FRET effect. Under the optimal conditions, the fluorescence response time was no more than 5 min, and the linear range of complex to MG was $0.5\text{--}25 \mu\text{mol L}^{-1}$ with a detection limit of $117.29 \text{ nmol L}^{-1}$. It was used as a fluorescent probe to detect MG in aquaculture water rapidly and accurately. The recoveries were in a range of 96.10–98.76%. This method has advantages including simple preparation, simple detection and rapid response. But this method has some disadvantages, such as poor selectivity and sensitivity. The successive

research work will focus on the enhancement of selectivity and sensitivity.

Acknowledgements

This research was supported by the Foundation from the Natural Science Foundation of Fujian Province of China (2018J01432, 2017J01633), the Open Foundation from Key Laboratory of Food Microbiology and Enzyme Engineering of Fujian Province (B18097-5), Cultivation Project in Jimei University for National Foundation (ZP2020029), and the National Undergraduate Training Programs for Innovation and Entrepreneurship (201910390017, 201810390024, 201710390300).

References

- Doerge D R, Chang H C, Divi R L and Churchwell M I 1998 Mechanism for inhibition of thyroid peroxidase by leucomalachite green *Chem. Res. Toxicol.* **11** 1098
- Sagar K, Malcolm R S, James G W and Kieran M 1994 High-performance liquid chromatographic determination of the triphenylmethane dye, malachite green, using amperometric detection at a carbon fibre microelectrode *J. Chromatogr. A* **659** 329

3. Lin Z Z, Zhang H Y, Li L and Huang Z Y 2016 Application of magnetic molecularly imprinted polymers in the detection of malachite green in fish samples *React. Funct. Polym.* **98** 24
4. Kumar P, Khosla R, Soni M, Deva D and Sharma S K 2017 A highly sensitive, flexible SERS sensor for malachite green detection based on Ag decorated microstructured PDMS substrate fabricated from Taro leaf as template *Sens. Actuat. B Chem.* **246** 477
5. Samanian K 2014 Identification of Green Pigment Used in Persian Wall Paintings (ad 1501–1736) Using PLM, FT-IR, SEM/EDX and GC-MS Techniques *Archaeometry* **57** 740
6. Sivashanmugan K, Liao J D, Liu B H, Yao C K and Luo S C 2015 Ag nanoclusters on ZnO nanodome array as hybrid SERS-active substrate for trace detection of malachite green *Sens. Actuat. B Chem.* **207** 430
7. Wu L, Lin Z Z, Zhong H P, Chen X M and Huang Z Y 2017 Rapid determination of malachite green in water and fish using a fluorescent probe based on CdTe quantum dots coated with molecularly imprinted polymer *Sens. Actuat. B Chem.* **239** 69
8. Yang J, Wu M H, Lin Z Z and Huang Z Y 2018 Detection of trace leucomalachite green with a nanoprobe of CdTe quantum dots coated with molecularly imprinted silica via synchronous fluorescence quenching *New J. Chem.* **42** 2640
9. Cao Y J, Wei J L, Wu W, Wang S, Hu X G and Yu Y 2015 Permethylated- β -Cyclodextrin Capped CdTe Quantum Dot and its Sensitive Fluorescence Analysis of Malachite Green *J. Fluoresc.* **25** 1397
10. Hanaoka K, Kikuchi K, Kobayashi S and Nagano T 2007 Time-resolved long-lived luminescence imaging method employing luminescent lanthanide probes with a new microscopy system *J. Am. Chem. Soc.* **129** 13502
11. Weibel N, Charbonnière L C J, Guardigli M, Roda A and Ziesel R 2004 Engineering of highly luminescent lanthanide tags suitable for protein labeling and time-resolved luminescence imaging *J. Am. Chem. Soc.* **126** 4888
12. Xu W, Zhou Y, Huang D, Su M, Wang K and Hong M 2014 A highly sensitive and selective fluorescent sensor for detection of Al(3+) using a europium(III) quinolinecarboxylate *Inorg. Chem.* **53** 6497
13. Wang X, Wang X, Wang Y and Guo Z 2011 Terbium(III) complex as a luminescent sensor for human serum albumin in aqueous solution *Chem. Commun.* **47** 8127
14. Wang B, Xiao L L, Xiang H X, Sun B and Zhu M F 2017 Enhanced Fluorescence Emission of Bonding Type Rare Earth Complexes Eu(MAA)₃Phen *Mater. Sci. Forum* **898** 1839
15. Barja B, Aramendia P, Baggio R, Garland M T, Peña O and Percec M 2006 Europium(iii) and terbium(iii) trans-2-butenates: syntheses, crystal structures, and properties *Inorg. Chim. Acta* **355** 183
16. Zaitoun M A and Al-Tarawneh S 2011 Effect of varying lanthanide local coordination sphere on luminescence properties illustrated by selected inorganic and organic rare earth complexes synthesized in sol-gel host glasses *J. Lumin.* **131** 1795
17. Liu H, Xu C, Bai Y, Liu L, Liao D and Liang J 2017 Interaction between fluorescein isothiocyanate and carbon dots: Inner filter effect and fluorescence resonance energy transfer *Spectrochim. Acta Part A* **171** 311
18. Biju V, Itoh T, Baba Y et al 2006 Quenching of Photoluminescence in Conjugates of Quantum Dots and Single-Walled Carbon Nanotube *J. Phys. Chem. B* **110** 2606
19. Lakowicz J R 1983 *Principles of Fluorescence Spectroscopy* (US: Springer)
20. Liu G S, Gong M L and Shi M L 2009 Synthesis and Luminescence of Eu(III) Complex Based on 4,4,4-Trifluoro-1-(4'-o-terphenyl)-1,3-butanedione and 1,10-Phenanthroline *Chin. J. Inorg. Chem.* **25** 828
21. Wei X, Meng M J and Song Z 2014 Synthesis of molecularly imprinted silica nanospheres embedded mercaptosuccinic acid-coated CdTe quantum dots for selective recognition of λ -cyhalothrin *J. Lumin.* **153** 326
22. Yang J, Wu H, Wu M H, Zeng J, Lin Z Z, Chen X M and Huang Z Y 2018 Simultaneous detection of malachite & leucomalachite green based on dual template CdTe@MIP via normal and synchronous fluorescence quenching *Dyes Pigm.* **155** 171